Supporting Information for:

NH$_3$ Binding to the S$_2$ State of the O$_2$-Evolving Complex of Photosystem II: Analog to H$_2$O binding during the S$_2 \rightarrow$ S$_3$ Transition

Mikhail Askerka, David J. Vinyard, Gary W. Brudvig and Victor S. Batista[*]

Department of Chemistry, Yale University, New Haven, Connecticut 06520-8107,

Section I. Description of QM/MM Models.

The choice of the high layer and the MM sphere was done according to the scheme described in our previous models.[1] We were able to optimize the two spin isomers of the S_2 state that give rise to g=2.0 and g=4.1 EPR signals. The main difference is the position of O5: in g=2.0 structure it is coordinated to Mn4 stabilizing oxidation states pattern III, IV, IV, IV; in the g=4.1 structure it is coordinated to Mn1 stabilizing oxidation states pattern IV, IV, IV, III. This is in agreement with previously reported computational models.[2]

Section II. EXAFS Analysis

Computational Details

FEFF 8.30[3] combined with IFEFFIT[4] v.1.2.11d programs were used to compute the EXAFS spectra of the S_1 and S_0 models. Only the QM layers were taken into account for computing the EXAFS of the QM/MM optimized structures. For the current calculations, we considered all paths with lengths up to eight scattering legs and the extremely small contribution from hydrogen atoms was not considered. A value of 0.003 Å for the Debye–Waller factors was employed in all calculations. The energy (E) axis was converted into photoelectron wave vector (k) space by using the following transformation; $k = (2m_e/(h/2\pi)^2)(E − E_0)$ where m_e is the mass of the electron and h is Planck's constant. A value of $E_0 = 6540.0$ eV for the Fermi energy has been employed for the calculations involving the QM/MM model. A fractional cosine-square (Hanning) window with $\Delta k = 1$ was applied to the k^3-weighted EXAFS data. The grid of k points, which are equally spaced at 0.05 Å^{-1}, was then used for the Fourier transformation (FT)

to R space. A k range of 4.2 − 10.6 Å^{-1} for the FT for the isotropic EXAFS data was employed. No The FT magnitude or EXAFS χk^3 scaling is used in the present study.

The predictive ability of simulated EXAFS was very recently assessed using multiple Mn complexes as well as structural data and computational models of the OEC.[5] In the present work, we use the structure of the OEC in the S_2 state in the native conditions as the reference. This model is in a very good agreement with the previously published model of S_2[2] and gives perfect agreement with EXAFS. This lets us explore various sites of ammonia binding under a fair assumption that those parameters will not change much upon binding of ammonia.

Wild-Type and Ammonia Bound S_2 EXAFS

In the EXAFS experiment, the main change of the spectrum upon ammonia binding is in the region from 7.5 to 11 $Å^{-1}$, where the well pronounced features in the control sample experience significant damping in the ammonia bound sample. The authors of the experimental work attribute this difference to elongation of one of the previously degenerate Mn-Mn distances from 2.72 Å to 2.87 Å using the two-shell fitting approach of the Fourier transform spectra.[6]
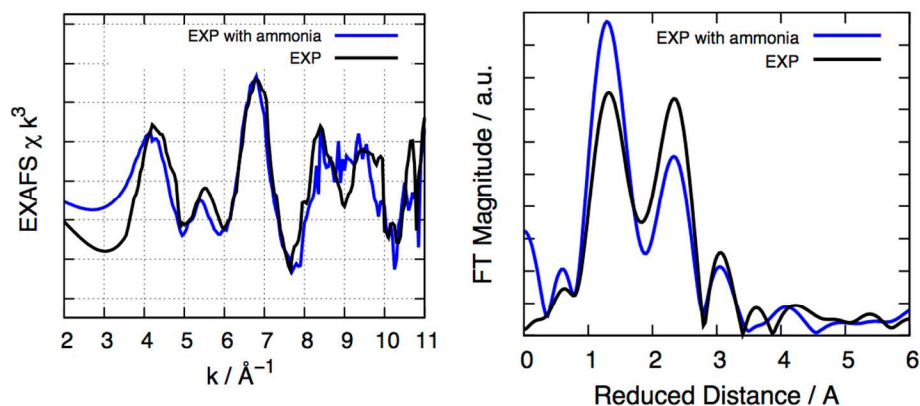

Figure S2. Experimental Mn EXAFS spectra on control (black) and ammonia-bound (blue) S-states of PSII in k-space (left panel) and reduced distance space (right panel). Data are from ref. 5.

EXAFS Simulation for Various Ammonia Binding Sites

We use the previously reported structure of the S_2 state[1] to explore the possibilities of ammonia adding to Mn4 or replacing a terminal water molecule bound to either Mn4 (W1, W2) or Ca (W3, W4) or ammonia replacing the O5 μ-oxo bridge in the form of amido (NH_2^-), imido (NH^{2-}) or nitrido (N^{3-}) ligands with the O4 μ-oxo bridge being either protonated (I_8-I_{10}) or not protonated (I_5-I_7). We use a comparison between simulated and experimentally obtained EXAFS[6] as a means to decide on the relevancy of

a particular binding site.

According to our QM/MM models, ammonia replacing terminal water molecules did not lead to any significant changes in the Mn-Mn distances within the OEC and, therefore, did not match the experimental EXAFS. The average change in Mn-Mn distance upon replacement of W1-W4 with NH_3 is 0.01 Å (I_1-I_4). This is expected given structural and electronic similarities between ammonia and water. There are significant changes (by as much as 0.63 Å) in the position of Ca and, therefore, Ca-Mn distances; however, they have almost no contribution to the spectrum because Ca acts only as a backscattering center.

Ammonia replacing the flexible O5 μ-oxo bridge is another widely discussed possibility for NH_3 binding. Here, we consider ammonia replacing the O5 μ-oxo bridge in the form of amido (NH_2), imido (NH) or nitrido (N) ligands. We also assume that upon replacing the O5 μ-oxo bridge ammonia can pass a proton to the nearby O4 μ-oxo bridge. Therefore, for each of the bridge motifs we also consider the O4 μ-oxo bridge to be singly protonated.

We find replacing the O5 μ-oxo bridge with ammonia leads to significant changes in the OEC cluster. The average Mn-Mn distance change is from 0.06 Å to 0.05 Å which, therefore, makes a visible difference in the EXAFS spectrum. The simulations show that replacing the O5 μ-oxo bridge with NH_2^- gives a reasonable agreement with EXAFS. Replacing an oxide ion with a bulkier NH_2^- ligand leads to an inflation of the region of the OEC around dangling Mn and, therefore, increases the Mn3-Mn4 distance by 0.14 Å leading to a distance of 2.84 Å. This result is not unexpected: it was predicted using the shell fitting method of Fourier transform EXAFS in the experimental work by Dau *et al.*[6];

the 2.84 Å distance is in also an agreement with a previously reported QM model.[7]

Although the NH_2^- ligand appears to be an attractive candidate at first sight, it has several drawbacks. First, one of the NH bonds of the NH_2^- species is pointing towards Ca making it impossible to form a Ca-N bond, which results in a dramatic increase in the Ca-N distance (by 0.87 Å) as shown in Table S1. Second, exchange of a μ-oxo bridge for NH_2^- is not isoprotonic and would imply a proton release that is not observed upon ammonia binding.

Achieving the desired intermetallic distances is also possible if we consider ammonia binding to the open cubane S_2 structure. The question of the isoprotonic exchange is erased if we then *add* ammonia (instead of *replacing*) as a 6th ligand to Mn4.

Table S1. Bond distances (Å) between the metal centers in the OEC of the QM/MM optimized structures with various motifs of ammonia binding. The color shows whether the distance increased (blue) or shortened (orange) by more than 0.05 Å with respect to the control S_2

| Motifs/ Distances			$\frac{Mn1}{Mn2}$	$\frac{Mn2}{Mn3}$	$\frac{Mn1}{Mn3}$	$\frac{Mn3}{Mn4}$	$\frac{Ca/Mn}{1}$	$\frac{Ca/Mn}{2}$	$\frac{Ca/Mn}{3}$
Control S_2		I_0	2.75	2.75	3.30	2.70	3.56	3.49	3.71
Terminal Sites	W1, open cubane	I_t	2.75	2.73	3.10	3.21	3.50	3.47	3.51
		I_t^{ref}	2.75	2.73	3.10	3.25	3.49	3.45	3.51
	W1	I_1	2.75	2.75	3.29	2.70	3.56	3.49	3.62
	W2	I_2	2.75	2.77	3.33	2.73	3.56	3.44	3.58
	W3	I_3	2.75	2.74	3.29	2.69	3.59	3.60	3.82
	W4	I_4	2.75	2.74	3.28	2.68	3.71	3.72	4.34
Bridging Sites: Replacing O5	O4 not protonated — NH_2	I_5	2.74	2.74	3.24	2.84	3.78	3.57	4.23
	NH	I_6	2.74	2.76	3.27	2.77	3.51	3.48	3.61
	N	I_7	2.74	2.75	3.03	2.59	3.37	3.39	3.48
	O4 protonated — NH_2	I_8	2.76	2.73	3.32	2.98	3.85	3.68	4.61
	NH	I_9	2.77	2.71	3.25	2.90	3.60	3.48	3.64
	N	I_{10}	2.78	2.74	3.19	2.72	3.46	3.46	3.85
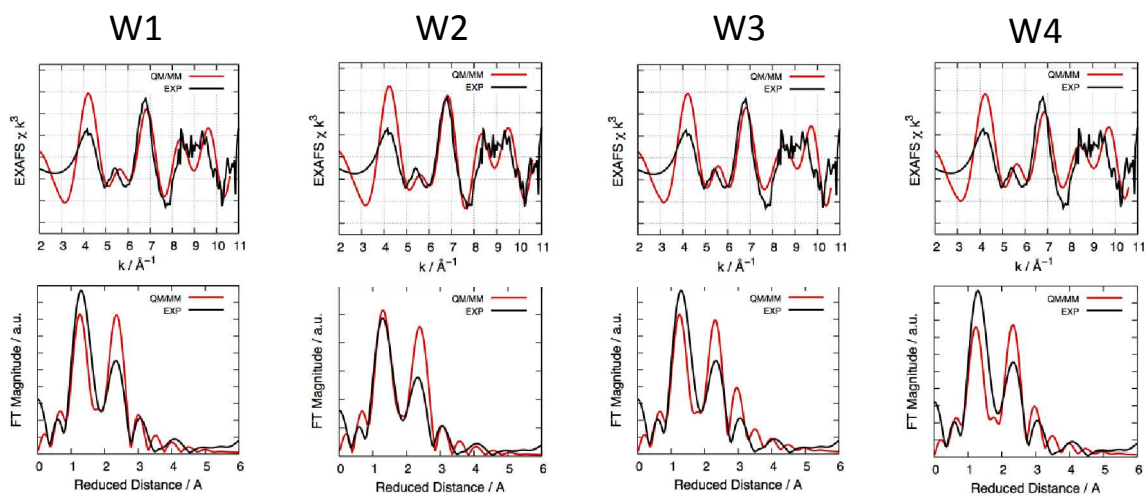
Figure S2. Overlay of calculated (red) and experimental (black) Mn EXAFS spectra in k-space and reduced distance space for the QM/MM optimized structures where ammonia replaces a *terminal* water molecule (W1-W4). Data are from ref. 5.
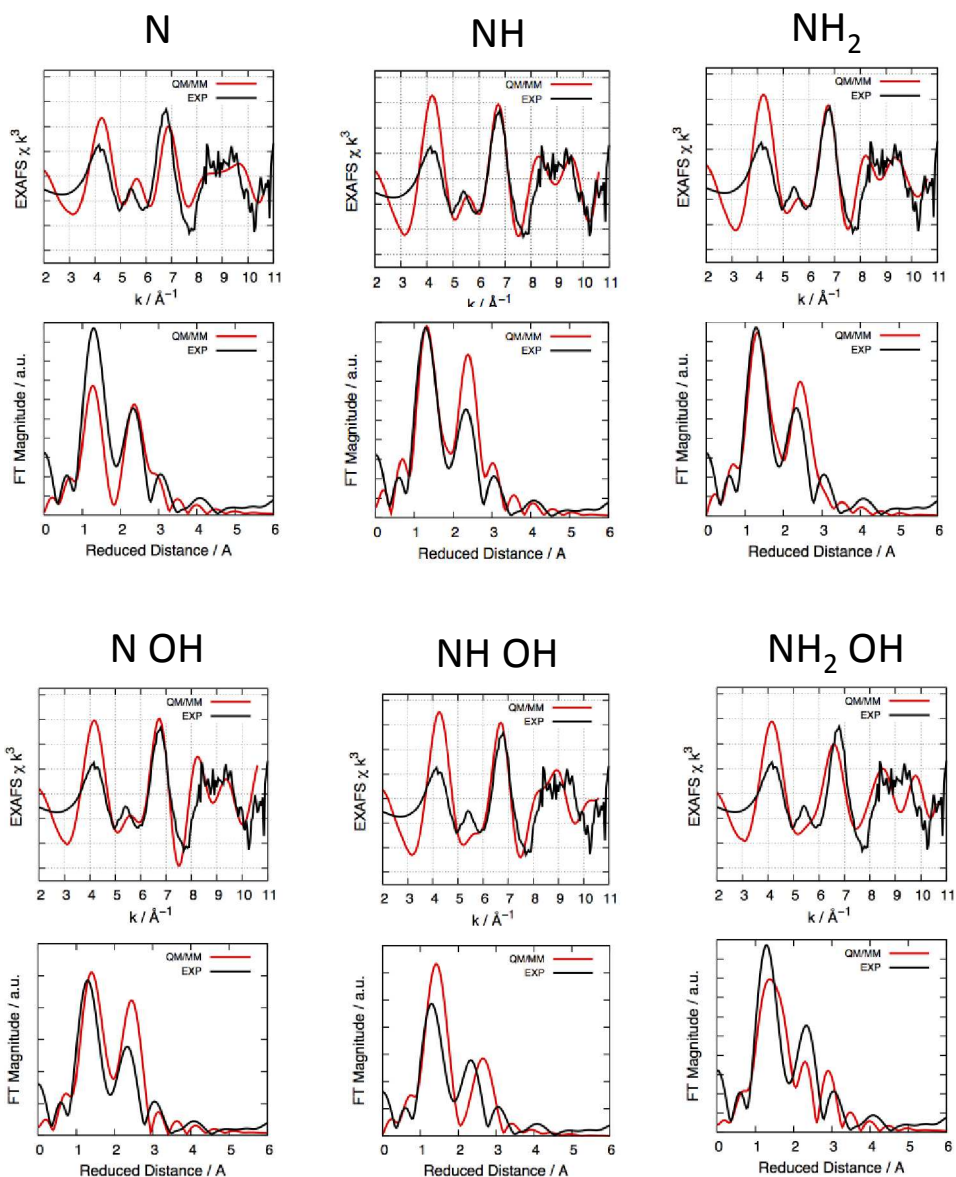
Figure S3. Overlay of calculated (red) and experimental (black) Mn EXAFS spectra in k-space and reduced distance space for the QM/MM optimized structures where ammonia replaces the *O5 µ-oxo bridge*. We considered various protonation states of ammonia (NH_2^-, NH^{2-}, N^{3-}) for protonated (denoted as OH) and not protonated (denoted as O) O4 µ-oxo bridge. Data are from ref. 5.

Section III: REFERENCES

[1] Askerka, M., Wang, J., Brudvig, G. W., and Batista, V. S. (2014) Structural Changes in the Oxygen-Evolving Complex of Photosystem II Induced by the S1 to S2 Transition: A Combined XRD and QM/MM Study, *Biochemistry 53*, 6860-6862.

[2] Pantazis, D. A., Ames, W., Cox, N., Lubitz, W., and Neese, F. (2012) Two Interconvertible Structures that Explain the Spectroscopic Properties of the Oxygen-Evolving Complex of Photosystem II in the S2 State, *Angew Chem Int Edit 51*, 9935-9940.

[3] Ankudinov, A. L., Bouldin, C. E., Rehr, J. J., Sims, J., and Hung, H. (2002) Parallel calculation of electron multiple scattering using Lanczos algorithms, *Phys Rev B 65*, 104107.

[4] Newville, M. (2001) IFEFFIT: interactive XAFS analysis and FEFF fitting, *J Synchrotron Radiat 8*, 322-324.

[5] Beckwith, M. A., Ames, W., Vila, F. D., Krewald, V., Pantazis, D. A., Mantel, C., Pecaut, J., Gennari, M., Duboc, C., Collomb, M. N., Yano, J., Rehr, J. J., Neese, F., and DeBeer, S. (2015) How accurately can Extended X-ray Absorption Spectra be Predicted from First Principles? Implications for Modeling the Oxygen-Evolving Complex in Photosystem II, *J Am Chem Soc*.

[6] Dau, H., Andrews, J. C., Roelofs, T. A., Latimer, M. J., Liang, W. C., Yachandra, V. K., Sauer, K., and Klein, M. P. (1995) Structural Consequences of Ammonia Binding to the Manganese Center of the Photosynthetic Oxygen-Evolving Complex - an X-Ray-Absorption Spectroscopy Study of Isotropic and Oriented Photosystem-Ii Particles, *Biochemistry 34*, 5274-5287.

[7] Schraut, J., and Kaupp, M. (2014) On Ammonia Binding to the Oxygen-Evolving Complex of Photosystem II: A Quantum Chemical Study, *Chem-Eur J 20*, 7300-7308.